Available online at www.sciencedirect.com
SCIENCE DIRECT
Polymer 46 (2005) 6402–6410
polymer
www.elsevier.com/locate/polymer

Making polyurethane foams from microemulsions

Christian Ligoure[a,b], Michel Cloitre[a,*], Christille Le Chatelier[a,c], Fabrice Monti[a], Ludwik Leibler[a]

[a]*Matière Molle et Chimie, UNRS CNRS-ESPCI 7167, ESPCI, 75231 Paris Cedex 05, France*
[b]*Laboratoire des Colloïdes, Verres et Nanomateriaux, UMR CNRS-UMZ 5587, Université Montpellier 2, 34095 Montpellier Cedex 05, France*
[c]*Physicochimie des Polymères et des Milieux Dispersés, UMR 7615, ESPCI, 10 rue Vauquelin, 75231 Paris Cedex 05, France*

Received 26 November 2004; accepted 12 April 2005
Available online 1 July 2005

Abstract

A remarkable correlation exists between the degree of expansion of polyurethane foams and the structure of the reacting premixes. Polyurethane foams obtained from reacting premixes containing microemulsions are highly expanded. The expansion rate is proportional to the volume fraction of microemulsion in the premix. The stability of premixes with and without microemulsion is completely different suggesting distinct creaming mechanisms. We apply this idea to synthesize polyurethane foams from microemulsions successfully. This approach can be used to rationalize the design of polyurethane formulations leading to highly expanded foams.

Keywords: Polyurethane; Foams; Microemulsion

1. Introduction

Polyurethane foams are one of the most important classes of cellular plastics [1]. The versatility of the polyurethane chemistry allows to produce a wide range of materials ranging from extremely soft flexible foams, through tough rigid foams, to films, fibers and molded devices, depending on the starting ingredients. Examples of applications are cushioning materials in furniture, bedding, carpet underlay, automobile and packaging.

Polyurethane foams result from the simultaneous polymerization of liquid monomers, which yields a cross-linked polymer network, and gas expansion [2]. Gas generation comes from blowing agents, for instance low boiling point liquids, which are purposely added into the system [3], or/and gases, such as carbon dioxide, which are produced by the reactants [2]. After reaction, we get a three-dimensional continuous polymeric phase throughout which gas cells are dispersed. The morphological characteristics of the cells and the level of expansion result from a delicate balance between the structuring of the reacting medium and the kinetics of gas bubble nucleation and growth [4]. The final properties of the foam result from both the geometry of the cells and the properties of the polymer forming the matrix [5].

A typical process for producing polyurethane foams at the laboratory scale involves two successive steps. In the first step, the monomers (polyols and polyesterols), the surfactants and the blowing agent are mixed together into a premix. The premix alone does not undergo any chemical reaction so that it can be stored during a long period. In a second step, cross-linking agents (diisocyanates) and catalysts are added to the premix. The polymerization reaction then takes place and simultaneously foaming begins. In real industrial processes, all the components are usually mixed together in a single step so that polymerization and foam expansion begin immediately.

The formulation of the premix and that of the final reactive mixture determine largely the technical performance of the final foam in terms of expansion rate, insulating properties and mechanical strength. Small variations of composition can affect the expansion rate of the foams. In particular, the nature of the surfactant and its concentration are two important parameters [6–9]. This is shown in Fig. 1 that presents photographs of polyurethane foams obtained

* Corresponding author. Tel.: +33 1 40 79 51 15; fax: +33 1 40 79 51 17.
E-mail address: michel.cloitre@espci.fr (M. Cloitre).

0032-3861/$ - see front matter © 2005 Elsevier Ltd. All rights reserved.
doi:10.1016/j.polymer.2005.04.089

Fig. 1. Photographs of polyurethane foams obtained from two premixes containing, respectively, 0.82 wt% (left) and 8.56 wt% (right) of surfactant. The percentages are expressed in g per 100 g of polyol.

from two different premixes. Both premixes contain the same basic ingredients; they only differ by the weight fraction of surfactant. The premix containing the largest amount of surfactant gives a highly expanded foam with small and homogeneously distributed cells. When the amount of surfactant is reduced, the expansion rate is smaller and the size distribution of the cells is broad with many large cavities.

In this paper, we show that this great variability of properties is associated with remarkable differences in the structure and the stability of the premixes itself. All premixes leading to 'good foams' systematically contain a microemulsion phase, which can be either a non-aqueous microemulsion (Sections 2–4) or an aqueous inverse microemulsion (Section 5). Moreover, we show that the volume fraction of microemulsion in the premix quantitatively controls the expansion rate of the final foams and many of their properties.

The paper is organized as follows. In Section 2, we present the materials and the methods. We describe a simple experimental set-up especially designed to study the stability and the creaming behavior of premixes. In Section 3, we demonstrate that only those premixes containing a microemulsion lead to well-expanded foams. We show that the foam density is inversely proportional to the volume fraction of microemulsion phase in the premix. The viscosity of the continuous phase of the premix has no effect. In Section 4, we study the creaming behavior of the premixes. We show that the kinetics of creaming is governed by the structure of the premix and by the polyol viscosity. We propose a simple model that allows us to estimate the size distribution of the droplets in the premixes. In Section 5, we apply these ideas to make polyurethane foams from microemulsions of hydroxylated polybutadiene in water. In Section 6, we discuss the scope of our results and we conclude.

2. Materials and methods

2.1. Products

The basic ingredients of polyurethane foams are polyol, isocyanates, catalysts, blowing agents, and surfactants.

In this study, we use commercially available polyols of trademark Terate® [10]. They are purchased from KOSA and used as received. Polyols of the series Terate2500® are aromatic hydroxy-terminated polyesters. They have the same chemical structure but different polymerization index. Their hydroxyl value [11] is 240 (mgKOH/g). The Terate® 2541L marks off from others by the addition of flame-retardants. The density and the viscosity of the Terate® polyols used in this study are given in Table 1. Since, they are totally miscible, it is possible to prepare mixtures with variable viscosities.

Hydroxyl-terminated polyesters react with diisocyanates to produce a cross-linked polyurethane network. The diisocyanate used in this study is diphenylmethane

Table 1
Physical properties of Terate® polyols

	Terate® 2541 8252-45	Terate® 2541 8252-44	Terate® 2541L EX8252-73
Specific density (kg/m^3)	1200	1200	1200
Viscosity (mPa s at 25 °C)	2877	5253	24218

diisocyanate (MDI) with an isocyanate index [12] of 300. The reaction is catalyzed by tertiary amines (Polycat 8 and AcK from Air Products).

The blowing agent used in the following is *n*-pentane (boiling point 36 °C, density: 0.6).

The surfactant is a polydimethylsiloxane polyether-graft copolymer, named L6900, purchased from Union Carbide.

2.2. Sample preparation

Foams are prepared as follows. We start with a premix made from polyol, *n*-pentane and surfactants. The different components are mixed together and stirred in a high-speed mixer during 3 min at 10,000 tr/mn. Two series of premixes have been prepared (Tables 2 and 3). In the first series (series E), the viscosity of the polyol is kept constant and the amount of surfactant is varied. In the second series (series B), the amount of surfactant is prescribed and the viscosity of the polyol is varied. Both series contain the same volume of *n*-pentane.

To make foams, we add diphenylmethane diisocyanate and catalysts to the premixes (32 g of MDI, 0.06 g of Polycat8, and 0.65 g of AcK for 18.7 g of polyol). The different ingredients are mixed together during 5 s with a turbine. The mixture is then poured in a cylindrical vessel. The reaction of polymerization of the polyol with the MDI begins immediately and simultaneously the foam expands freely in the container. The foaming process is fast (2–3 min), highly exothermic and involves a large volume increase.

2.3. Experimental set-up and data analysis

When kept at rest, premixes are not stable and separate into different phases. In the following, we show that there is a direct relation between the final properties of the foam and the stability and the structure of the premixes. We have studied the kinetics of phase separation and measured the volume of the different phases at thermodynamic equilibrium by image analysis using a home-built experimental set-up. The cylindrical test tube containing the premix is put in a glass vessel filled with water in order to minimize the geometric distortions. It is uniformly lighted from behind. A CCD camera connected to an image grabber takes images of the tube. The different phases are simply identified from their luminance: the transparent *n*-pentane phase has a high luminance, whereas the brown polyol phase has a low luminance. Profiles of luminance along the vertical direction are obtained by averaging the luminance measured along 50 vertical lines parallel to the long axis.

3. Relation between the structure of premixes and foam expansion

3.1. Structure of premixes prepared without surfactant or with a fluorinated surfactant

Let us first investigate the stability of premixes prepared without surfactant. Fig. 2(a) shows premix E_1 after a few days. Two phases coexist. The upper phase is transparent and colorless: it mainly contains *n*-pentane. The bottom phase is viscous and brown: its major component is polyol.

Fig. 2(b) shows the profile of luminance that is measured experimentally along the vertical direction. The meniscus between air and *n*-pentane is revealed by a shallow minimum in the luminance profile. It defines the origin of the vertical axis, which is directed downwards. The bottom of the test tube is situated at $z=L$. The *n*-pentane phase and the polyol phase have a constant luminance. They are separated by a sharp interface at the vertical coordinate $z=H$. For $z>0$, the experimental profile of luminance is well described by:

$$I(z) = I_0 + I_1 \tanh\left(\frac{z-H}{\delta}\right) \quad (1)$$

where I_0 and I_1 can be expressed in terms of the luminance of the *n*-pentane and polyol phases; δ is the derivative of $I(z)$ at $z=H$. With this method, it is possible to locate the vertical position of the *n*-pentane/polyol interface accurately.

These results show that premixes prepared without surfactant are unstable emulsion comprising droplets of *n*-pentane dispersed in a continuous polyol phase. Upon

Table 2
Composition of the premixes of the series E

	E_1	E_2	E_3	E_4	E_5	E_6	E_7
Polyol	100	100	100	100	100	100	100
L6900	0	0.062	0.82	1.71	4.28	5.89	8.56
n-Pentane	23.8	23.8	23.8	23.8	23.8	23.8	23.8

The quantities are expressed in g per 100 g of polyol.

Table 3
Composition of the premixes of the series B

	B_1	B_2	B_3	B_4	B_5
Polyol viscosity (mPa s)	2877	3827	4302	5253	9000
Polyol 8252-73	0	0	0	0	20
Polyol 8252-44	0	40	60	100	80
Polyol 8285-45	100	60	40	0	0
L6900	4.278	4.278	4.278	4.278	4.278
n-Pentane	23.8	23.8	23.8	23.8	23.8

The different quantities are given in grams.

creaming, the premixes separate into polyol and *n*-pentane. We have found the same behavior in premixes prepared with a fluorinated surfactant that is insoluble both in *n*-pentane and in polyol.

3.2. Structure of premixes prepared with a silicone surfactant

In this paragraph, we study the creaming equilibrium of premixes E_2–E_7 prepared with the silicone surfactant. Fig. 3(a) shows premix E_5 at thermodynamic equilibrium. Now we can distinguish three phases. The upper phase is transparent and colorless: it mainly contains *n*-pentane. The bottom phase is viscous and brown: its major component is polyol. The intermediate phase is transparent but slightly colored suggesting that it is a submicron dispersion of polyol in *n*-pentane.

Fig. 3(b) shows the profile of luminance that is measured experimentally along the vertical direction. Again, the meniscus between air and *n*-pentane is revealed by a shallow minimum in the luminance profile. This defines the origin of the vertical axis, which is directed downwards. The bottom of the test tube is situated at $z=L$. The three phases are separated by two sharp interfaces at $z=H$ and $z=H'$. To measure their volume, we generalize the procedure described in the previous section, fitting the experimental profile of luminance to the expression:

$$I(z) = I_0 + I_1 \tanh\left(\frac{z-H}{\delta}\right) + I_2 \tanh\left(\frac{z-H'}{\delta'}\right) \quad (2)$$

I_0, I_1 and I_2 are functions of the luminance of the different phases; $1/\delta$ and $1/\delta'$ are the derivatives of $I(z)$ at $z=H$ and $z=H'$.

We have studied the structure of the intermediate phase by small angle X-ray scattering. The scattering experiments have been performed on the ID2 beam-line at the ESRF. The samples have been prepared by removing the intermediate phase from the premixes with a syringe. An example of scattering pattern is shown in Fig. 4. It exhibits a smooth correlation peak centered on wave vector q^*. This peak is characteristic of a liquid-like order with a mesoscopic correlation length ξ of the order of 10 nm ($\xi=2\pi/q^*$). This results shows that the intermediate phase is a microemulsion of polyol in *n*-pentane stabilized by silicone surfactant. Since, the microemulsion coexists with two immiscible phases, it must be of Winsor III type [13].

3.3. Relation between the microemulsion phase and foam expansion

In Fig. 5, we plot the volume fraction of the

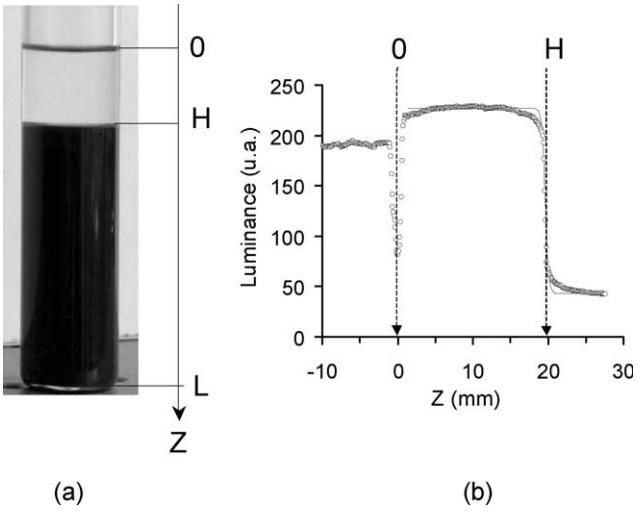

Fig. 2. Creaming behavior of premix E_1, (a) photograph showing the premix at equilibrium, (b) profile of luminance measured experimentally (open dots) and best fit (continuous line) of the experimental data to Eq. (1).

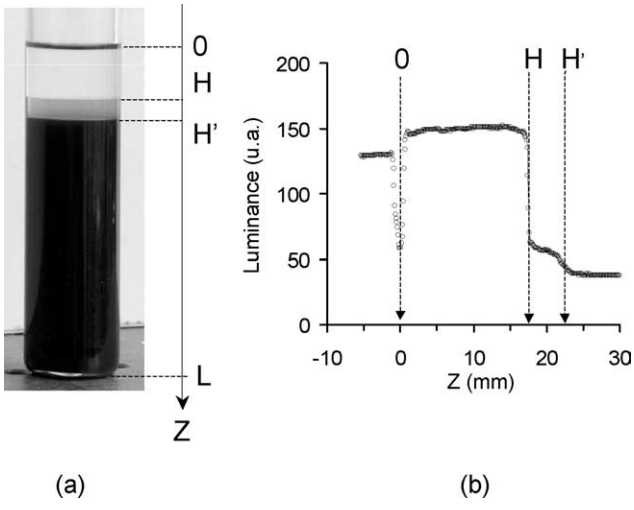

Fig. 3. Creaming behavior of premix E_5, (a) photograph showing the premix at equilibrium, (b) profile of luminance measured experimentally (open dots) and best fit (continuous line) of the experimental data to Eq. (2).

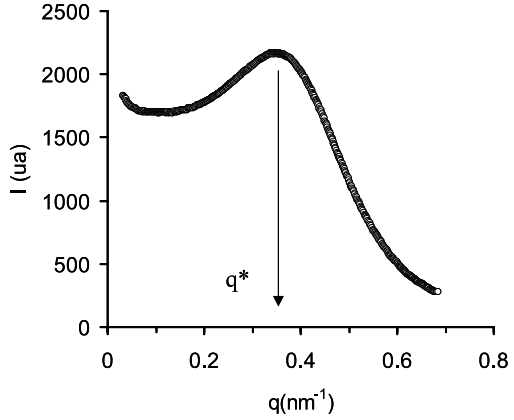

Fig. 4. SAXS spectrum of the intermediate phase extracted from premix E_5.

microemulsion phase at thermodynamic equilibrium versus the weight fraction of surfactant for the premixes of series E. The volume fraction of the microemulsion phase, Φ, is obtained from H and H' through the relation: $\Phi=(H'-H)/L$. We observe that the volume fraction of the microemulsion is proportional to the weight fraction of surfactant.

In Fig. 6, we plot the density of the foams obtained after expansion versus the weight fraction of surfactant in the premixes. We observe that the volume of the foam is also proportional to the weight fraction of surfactant in the premixes. The foam made from the premix containing 8% of surfactant is 2.5 times more expanded that the foam obtained from the premix containing 2% of surfactant. It is interesting to compare these experimental results with the theoretical density ρ_{min} that would be reached if all the *n*-pentane added to the formulation were to contribute to the foam expansion. ρ_{min} is estimated from the composition of the foaming mixtures and the material properties of the different components in Appendix A. Fig. 6 shows that the actual density of the foams is systematically larger than the theoretical density ρ_{min} that is expected from the volume

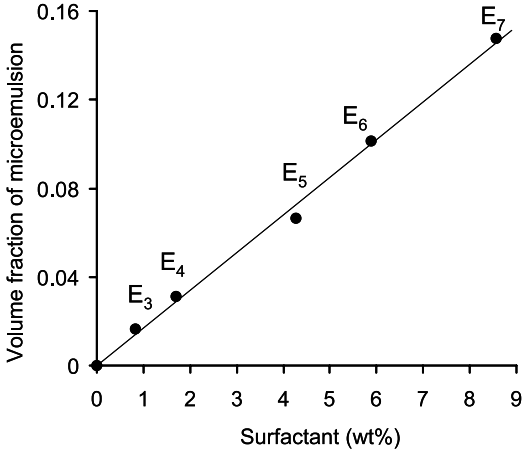

Fig. 5. Volume fraction of microemulsion versus surfactant concentration (series E). The surfactant concentration is given in g per 100 g of polyol. The volume fraction of the microemulsion in premix E_2 is within the experimental accuracy.

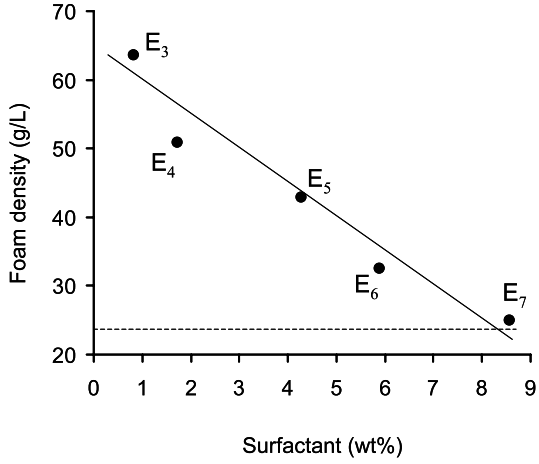

Fig. 6. Density of final foams versus surfactant concentration (series E). The density of the foam obtained from premix E_2 cannot be determined reliably. The dotted line represents the density expected if the entire blowing agent were incorporated into the foam (Appendix A).

of blowing agent in the premix. Only at the largest surfactant concentration, the foam density approaches the maximum value ρ_{min}. This shows that only a fraction of the blowing agent added to the premix contributes to the foam expansion. Interestingly, this fraction is directly related to the volume fraction of microemulsion in the premix.

Let us now consider premixes of the series B (Table 3), where we have kept the surfactant weight fraction constant and we have varied the viscosity of the continuous phase.

At thermodynamic equilibrium the volume fractions of the polyol, *n*-pentane and microemulsion phases are the same for all the samples of the series. The density of the foams obtained after expansion is also roughly constant in the range 40–48 kg/m^3.

In conclusion, the expansion rate of polyurethane foams is proportional to the volume fraction of premix that is micro-organized at thermodynamic equilibrium. It does not depend directly on other parameters such as the quantity of blowing agent in the premix or the viscosity of the reactants.

4. Kinetics of creaming

The existence of a microemulsion in a premix is associated with specific creaming properties. In the following, we show that this can be used as a useful test to evaluate the performance of polyurethane foam formulations.

4.1. Creaming of premixes with and without microemulsion

Fig. 7 shows the profiles of luminance measured during creaming of premix E_1, which does not contain microemulsion. At short times, the contrast between the different phases is blurred by the presence of a film of polyol flowing down slowly along the walls of the test tube. However,

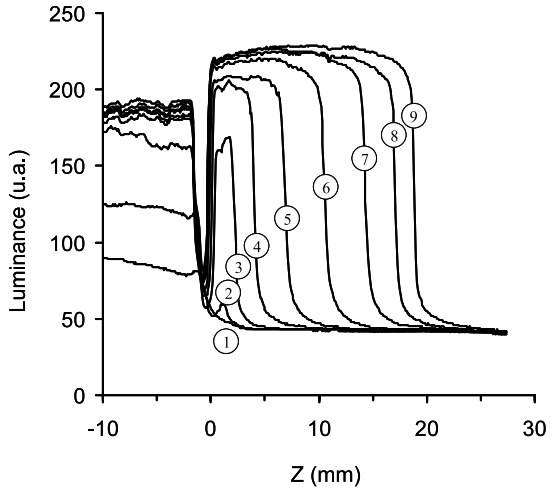

Fig. 7. Profiles of luminance measured experimentally during the creaming of premix E_1. The different profiles are taken at: $t=12$ mn (1), 24 mn (2), 84 mn (3), 144 mn (4), 204 mn (5), 264 mn (6), 324 mn (7), 384 mn (8), 944 mn (9). The time origin is taken at the end of the initial mixing of the ingredients. Note that a thin layer of pentane forms very rapidly.

immediately after preparation, a thin layer of *n*-pentane can be distinguished and an interface between *n*-pentane and polyol can be detected. This interface moves downwards with time. After $t=2\times10^4$ s, the appearance of the premix does not change significantly indicating that creaming is complete.

Fig. 8 shows that the existence of a microemulsion in a premix is associated with a completely different behavior. We have represented the profiles of luminance measured during creaming of premix E_5. Initially, the premix appears uniformly brown without any phase separation. Only after a lag time of about 5×10^3 s, it is possible to distinguish a thin layer of pentane at the top of the premix. The microemulsion appears later. After typically 6×10^4 s, the profiles of luminance no longer evolve indicating that creaming is complete. Premixes E_2–E_7, which all contain a microemulsion, have the same behavior except premix E_2 for which there is no lag time.

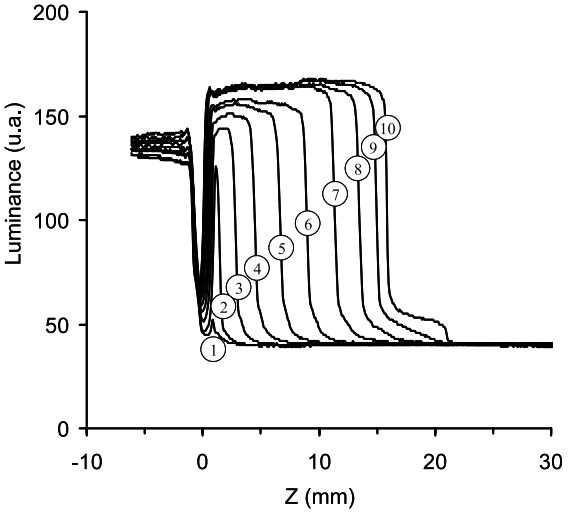

Fig. 8. Profiles of luminance measured experimentally during the creaming of premix E_5. The different profiles are measured at: $t=84$ mn (1), 96 mn (2), 108 mn (3), 1204 mn (4), 138 mn (5), 168 mn (6), 228 mn (7), 330 mn (8), 474 mn (9), 1134 mn (10). The time origin is taken at the end of the initial mixing of the ingredients. Note that the layer of *n*-pentane forms after a lag time.

4.2. Determination of the creaming velocity

In the following, we characterize the kinetics of creaming by the variations of the quantity $H(t)$ defined in Figs. 2 and 3. $H(t)$ represents the vertical position of the interface between *n*-pentane and polyol (premixes without microemulsion) or that of the interface between *n*-pentane and the microemulsion (premixes with microemulsion). To compare easily the different premixes, it is convenient to normalize $H(t)$ by its asymptotic value H_∞ measured at thermodynamic equilibrium and to plot $H(t)/H_\infty$ as a function of t (for E_1 and E_2) or $t-t_{lag}$ (for E_3–E_7).

The results are shown in Fig. 9. It is interesting to compare the kinetics of creaming of the different premixes. In the case of E_1, $H(t)/H_\infty$ first increases linearly then exhibits a slight upwards curvature indicating that creaming becomes faster at long times. The value of the initial velocity, $U(0)=(dH/dt)_{t=0}$, is about 6×10^{-4} mm/s. The result obtained for E_2 is significantly different. At short times, the curve is nearly superimposed to that measured for E_1, indicating that the initial creaming velocity is not changed. At long times, however, $H(t)$ approaches its equilibrium value very slowly indicating that the creaming velocity becomes very small. The variations of $H(t)/H_\infty$ for

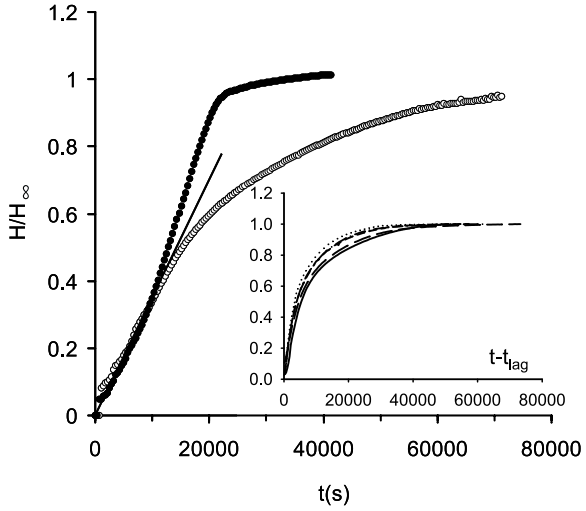

Fig. 9. Variation of $H(t)/H_\infty$ during the creaming of premixes E_1–E_7 ($H(t)$ is defined in Figs. 2 and 3, H_∞ is the value of $H(t)$ at equilibrium). The origin of the vertical axis is taken at the air/*n*-pentane interface. The main graph compares the variations measured for E_1 (●) and E_2 (○) The slope of the continuous line gives the initial creaming velocity. The inset shows the results obtained for E_3 (solid line), E_4 (long dashed line), E_5 (short dashed line), E_6 (dash-dot line), E_7 (dotted line). Note that the data in the inset are plotted versus $t-t_{lag}$.

premixes E_3–E_7 are shown in the inset of Fig. 9. Again we can define an initial creaming velocity $U(0)$. $U(0)$ increases slightly with the surfactant concentration from $U(0)=1.3\times 10^{-3}$ mm/s for E_3 to $U(0)=1.7\times 10^{-3}$ mm/s for E_7. It is interesting to note that these values are significantly larger than the initial velocity found for E_1 and E_2. The creaming velocity becomes very small in the late stages.

In Fig. 10 we analyze the role of the viscosity of the continuous phase. The inset shows the variations of $H(t)/H_\infty$ versus $t-t_{lag}$ for the premixes of the series B. All the curves have the same shape. However, the kinetics of creaming depends directly on the polyol viscosity: the greater polyol viscosity, the slower creaming. To be more quantitative, we have plotted the variations of $H(t)/H_\infty$ as a function of $\eta_0(t-t_{lag})/\eta$, where η_0 is the viscosity of B_1 chosen as a reference viscosity ($\eta_0=2877$ mPa s) and η is the viscosity of polyol in the premix. In this representation, all the curves collapse within the experimental accuracy. This result shows that the creaming velocity is simply proportional to the viscosity of the continuous phase.

4.3. Discussion

The creaming behavior of premixes prepared without surfactant suggests that the droplet size distribution is not too broad and that it is possible to define an average effective size. Indeed, the creaming of an emulsion is formally equivalent to the sedimentation of a suspension [14] when phenomena like coalescence between droplets, Oswald ripening, and depletion flocculation can be neglected. Droplets move up at the top of the emulsion under the combined action of buoyancy, hydrodynamic and thermodynamic forces. Here, we shall assume that the droplets of pentane are sufficiently large to neglect

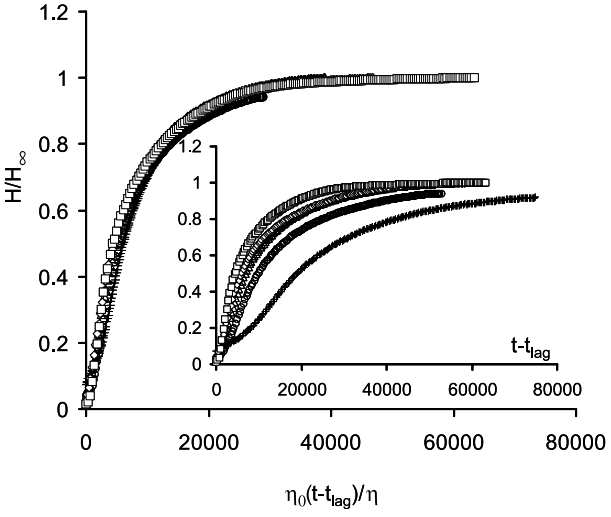

Fig. 10. Variation of $H(t)/H_\infty$ during the creaming of premixes B_1 (□), B_2 (■), B_3 (△), B_4 (×) and B_5 (+). $H(t)$ is defined in Figs. 2 and 3, H_∞ is the value of $H(t)$ at equilibrium. The inset shows the raw data plotted versus $t-t_{lag}$. In the main graph, $t-t_{lag}$ is normalized by the ratio between the current viscosity and the reference viscosity $\eta_0=2877$ mPa s.

diffusion. At infinite dilution, a droplet of *n*-pentane of radius a in polyol rises upwards at a constant velocity $U_0(a)$ that results from the balance between the Stokes force and the buoyancy force:

$$U_0 = \frac{2}{9}\frac{\Delta\rho g a^2}{\eta} \tag{3}$$

where η is the polyol viscosity. At finite concentrations, the droplet experiences the backflow due to the motion of its neighbors. The velocity now depends on the volume fraction of droplets, φ, through a coefficient $K_0(\varphi)<1$:

$$U(\varphi) = U_0 K_0(\varphi) \tag{4}$$

Different forms have been proposed for $K_0(\varphi)$. In the following, we shall use the Richardson–Zaki empirical formula which is known to describe the sedimentation of concentrated suspensions [14]: $K_0(\varphi)=(1-\varphi)^{-5.5}$. The mean radius of the droplets can be estimated easily from relation (4). For sample E_1 we find $a\cong 130$ μm. In this approach, we have neglected coalescence, which is likely to occur in the late stages of creaming. In that case, a should be considered as the effective particle size and not as the actual particle size in the premix.

The creaming behavior of premixes prepared with a silicone surfactant can be understood by considering that the main effect of the surfactant is to stabilize small droplets, leading to very polydisperse premixes with large and small droplets coexisting and creaming simultaneously. In such a polydisperse emulsions, droplets of different sizes rise at different velocities. Large droplets, which rise more quickly than small droplets, create a large backflow, which slows down the small droplets [14,15]. By contrast, the backflow created by the small droplets is negligible, so that the large droplets tend to rise faster than in a monodisperse emulsion. This may explains why the initial creaming velocity increases with the surfactant concentration and why creaming is slower in the presence of surfactant. It has been shown that this effect is particularly important for multimodal size distribution and for very broad size distributions [15].

Finally, the fact that the creaming velocity is proportional to the polyol viscosity implies that the droplet size distribution is independent of the viscosity of the continuous phase. This is a consequence of the fact that emulsions are prepared by turbulent mixing at high capillary number [16].

In conclusion, the presence of a microemulsion in a premix is associated with a very broad droplet size distribution that depends only on the initial mixing of the premix and the quantity of surfactant.

5. Making polyurethane foams from microemulsions

In view of the previous result, it is of fundamental interest to synthesize polyurethane foams from

microemulsions. The difficulty is to find a surfactant able to stabilize a microemulsion of blowing agent in polyol over a wide range of composition. In the following, we adopt the following procedure. Again, we start from a hydroxyl-terminated compound that reacts with a di-functional MDI to form a three-dimensional polyurethane network. This hydroxyl terminated reactant is a hydroxylated polybutadiene commercially available from Arkema under the trademark PolyBd® R20LM. The diisocyanate is MDI DNR from ICI. In the presence of water, diisocyanates react and release CO_2, which acts as a blowing agent:

$$2O{=}C{=}N{-}R{-}N{=}C{=}O + H_2O$$

$$\rightarrow O{=}C{=}N{-}R{-}NH{-}CO{-}NH{-}R{-}N{=}C{=}O + CO_2$$

Therefore, it is possible to get a polyurethane foam from a mixture of PolyBd®, MDI, water and a surfactant. It turns out that premixes made of PolyBd®, water and soya bean lecithin form microemulsions at least in a limited range of the ternary diagram. Lecithin is a natural surfactant that is known to form inverse microemulsions in many organic/water mixtures [17]. The lecithin used in this study is Epikuron 200 commercially available from Lucas Meyer.

The experimental protocol is the same as before. PolyBd®, MDI and lecithin are mixed together using a high-speed mixer. The premix is a transparent, homogeneous yellowish solution. Catalysts (Polycat 8) and MDI are added in a second step. The polymerization reaction and the foaming process begin immediately. We have prepared different foams according to Table 4 and we have measured the density of each of them.

The results are shown in Fig. 11. As expected the density decreases, i.e. the expansion rate increases, with the quantity of water in the premix. It is interesting to compare these results with the maximum expansion rate that would be obtained if all the water introduced in the formulation were to contribute to the expansion. This maximum expansion rate can be estimated using the method presented in the Appendix A by noting that 1 mol of water yields 1 mol of blowing agent according to the above reaction. The results are compared with the experimental data in Fig. 11. They differ drastically from those shown in Fig. 7. Now the variations of the maximum expansion rate follow closely the experimental data. Everything happens just as if all the water dispersed in the microemulsion were to contribute effectively to the expansion of the foam. Here, further expansion of the foam is restricted by the amount of blowing and not by the efficiency of the foaming process itself.

Table 4
Composition of the reactive premixes used to make polyurethanes foams from microemulsions

	L_1	L_2	L_3	L_4
Water	0.138	0.264	0.39	0.516
PolyBd®R20LM	40	40	40	40
MDI DNR	18.5	18.5	18.5	18.5
Lecithin	1.2	1.2	1.2	1.2
Polycat	0.4	0.4	0.4	0.4

The different quantities are given in grams.

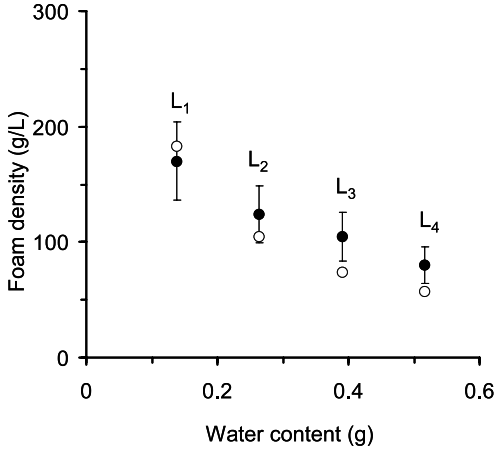

Fig. 11. Density of final foams versus water content for foams obtained from PolyBd® R20LM-water-Lecithin microemulsions (series L). The full dots refer to the experimental data. The open dots represent the maximum foam expansion that can be reached (Appendix A).

6. Concluding remarks

In this study, we have obtained several important results:

(1) A remarkable correlation exists between the degree of expansion of polyurethane foams and the structure of the reacting mixtures. The presence in the premixes of a microemulsion phase coexisting with polyol and *n*-pentane is necessary to achieve high expansion rates.
(2) The expansion rate of foams is proportional to the volume fraction of premix that is micro-organized at equilibrium. The latter is itself proportional to the weight fraction of surfactant and does not depend on other parameters like the polyol viscosity or the quantity of blowing agent.
(3) The creaming behavior of bad and good emulsions is completely different suggesting distinct droplet size distributions and different creaming mechanisms. This may provide useful guides to test the potential foaming quality of a formulation.
(4) The creaming behavior of a premix containing a microemulsion suggests that the role of the surfactant is two-fold. First, it contributes to emulsify the blowing agent into the continuous phase, leading to a highly polydisperse droplet size distribution. Secondly, it allows the mixing of the two components at the nanometer scale through forming a thermodynamically stable microemulsion.

We think that the presence of a microemulsion is important for at least two reasons. On one hand, the nanodroplets of the dispersed phase act as nucleating centers

from which bubble growth is initiated. These domains are remarkably stable with respect to buoyant forces and surface forces. On the other hand, the droplets of the microemulsion have a much larger surface/volume ratio than the emulsion droplets. Therefore, they act as a reservoir of surfactant molecules that is able to stabilize efficiently the bubbles of blowing agent during their expansion. The diffusion of surfactant molecules from the reservoir to the interfaces of the bubbles contributes to maintain a low surface tension and a low-pressure difference between bubbles of different sizes, thereby suppressing bubble coalescence. The presence of a microemulsion in the liquid films between two bubbles increases their viscosity and retards the thinning of the films by drainage and cell opening.

Our results suggest a new approach to optimize the formulation of polyurethane foams: the best formulation should involve a premix (consisting of polyol, surfactant and blowing agent) with a phase diagram exhibiting a large domain of microemulsion phase stability. We have already applied successfully this idea to synthesize polyurethane foams from a mixture of hydroxylated polybutadiene, water, surfactant and diisocyanate, where the ternary system polybutadiene-water-surfactant is a stable microemulsion. The blowing agent is carbon dioxide produced during the reaction of water with diisocyanates.

This approach should be useful in many other situations whenever efficient foaming is a key to success: food chemistry, biological synthetic materials. In that respect designing well-balanced surfactants able to stabilize microemulsions in complex formulations is a crucial issue. Recent work in that direction might provide a useful and systematic methodology [18].

Acknowledgements

The authors thank Dr Arnaud Albouy from Arkema for this interest in this work and his help during the experiments. We are indebted to Dr Pierre Panine for his help during the SAXS experiments. Christian Ligoure thanks the company Arkema for partial financial support.

Appendix A. Calculation of the maximum foam expansion

We assume that foam expansion is due entirely to the presence of gaseous *n*-pentane in the foam. In particular, we neglect the contribution of air that can be incorporated in the reacting mixtures during preparation. Then, the specific gravity of foams at maximum expansion, $\rho_{\min}$, can be estimated from the relation:

$$\rho_{\min} = \frac{M_P + M_I + M_C + M_S + m_P}{V_G + M_P/\rho_P + M_I/\rho_I + M_C/\rho_S + M_S/\rho_S}$$

M_P, M_I, M_C, M_S and m_P are, respectively, the mass of polyol, of MDI, of catalysts, of surfactants and of *n*-pentane in the foaming mixture. ρ_P, ρ_I, ρ_C, and ρ_S are the specific gravity of polyol ($\cong 1.2$ g/cm^3), of MDI ($\cong 1.2$ g/cm^3), of catalysts, and of surfactants. ρ_C and ρ_S are of the order of 1 g/cm^3. V_G is the volume of *n*-pentane in the final foam. In the following, we assume that there is no loss during the foaming process and that the expansion is not impeded by the reaction of polymerization. Then V_G is the volume of *n*-pentane under the conditions of polymerization ($P = 1$ atm and $T = 170$ °C). V_G is estimated directly from the law of perfect gases.

We use a similar approach to predict the expansion of foam obtained from hydroxylated polybutadiene in Section 5.

References

[1] Oertel G. Polyurethane foams. Munich: Hanser Publishing; 1993.
[2] Artavia L, Macosko CW. Low density cellular plastics, physical basis of behavior. In: Hilyard NC, Cunningham A, editors. London: Chapman and Hall [Chapter 2].
[3] Singh SN. Blowing agents for polyurethane foams. Shropshire, Midlands, UK: Rapra Technology; 2002.
[4] Herrington RM, Turner RB. In: Frisch KC, Klempner D, editors. Advances in urethane science and technology, vol. 12. Lancaster, PA: Technomic Pub; 1992.
[5] Gibson LJ, Ashby MF. Cellular solids: structure and properties. Cambridge: Cambridge University Press; 1999.
[6] Biesmans G, Colman L, Vandesande R. J Colloid Interf Sci 1998;199:140–50.
[7] Krupers MJ, Bartelink CF, Grünhauer HJM, Möller M. Polymer 1998;39:2049–53.
[8] Zhang XD, Macosko CW, Davis HT, Nikolov AD, Wasan DT. J Colloid Interf Sci 1999;215:270–9.
[9] Kaushiva BD, McCartney SR, Rossmy GR, Wilkes GL. Polymer 2000;41:285–310.
[10] More technical information is available at http://www.kosa.com/poly/specprod.htm
[11] The hydroxyl value represents the average weight fraction of hydroxyl groups in the polyol molecule. The hydroxyl value is obtained from the mass of potassium hydroxide (expressed in mg) necessary to neutralize the acetic anhydride that would react with 1 g of polyol.
[12] The isocyanate index represents the excess of isocyanate with respect to the stoechiometric conditions that is necessary to obtain total reaction.
[13] Clausse M. In: Becher P, editor. Encyclopedia of emulsion technology, vol. 1. New York: Marcel Dekker; 1983. p. 639–47.
[14] Russel WB, Saville DA, Schowalter WR. Colloidal dispersions. Cambridge: Cambridge University Press; 1989.
[15] Esipov SE. Phys Rev E 1995;52:3711–8.
[16] Walstra P. In: Becher P, editor. Encyclopedia of emulsion technology. New York: Marcel Dekker; 1983 [Chapter 2].
[17] Luisi PL, Scartazzani R, Haering G, Schurtenberger P. Colloid Polym Sci 1990;268:356–74.
[18] Lee JH, Balsara NP, Krishnamoorti R, Jeon HS, Hammouda B. Macromolecules 2001;34:6557–60.